Supporting information for

KCTD10 regulates brain development by destabilizing brain disorder-associated protein KCTD13

Jianbo Cheng[1#], Zhen Wang[1#], Manpei Tang[1#], Wen Zhang[1#], Guozhong Li[1#], Senwei Tan[1], Chenjun Mu[1], Mengyuan Hu[1], Dan Zhang[3], Xiangbin Jia[1], Yangxuan Wen[1], Hui Guo[1,2], Dan Xu[4], Liang Liu[5], Jiada Li[1,2], Kun Xia[1,2], Faxiang Li[1,2], Ranhui Duan[1,2], Zhiheng Xu[3,1]*, Ling Yuan[1,2]*

* Corresponding authors: Ling Yuan, Zhiheng Xu

Email: yuanling@sklmg.edu.cn (YL)

zhxu@genetics.ac.cn (ZX)

This PDF file includes:

Supplemental Methods and Materials

Figures S1 to S8

Table S1 and S2

Video S1 legend

Supplemental Methods and Materials

Plasmids

The cDNA encoding Human KCTD10 and KCTD13 that was used as a template for plasmid construction was a gift from Dr. Jiahuai Han. The KCTD10-encoding gene was PCR amplified and inserted into the pEGFP-C1 vector between the EcoRI and BamHI restriction sites or the pCMS-EGFP vector between the EcoRI and XbaII sites. The pCMS-EGFP-KCTD10 truncation plasmids (ΔIDR, ΔBTB, and ΔPCNA) were generated by site-directed mutagenesis PCR using KOD-Plus-Neo polymerase (ToYoBo). In addition, Human *KCTD13* cDNA was PCR amplified and subcloned into the pmCherry-C1 vector between the EcoRI and BamHI sites and the pcDNA3.1-HA vector. All constructs were confirmed by DNA sequencing.

Cell culture and plasmid transfection

HEK293T and NIH3T3 cells (ATCC) were maintained in DMEM (Gibco) supplemented with 10% fetal bovine serum (FBS, Gibco) at 37 ˚C with 5% CO_2. NIH3T3 cells were seeded on coverslips in 24-well plates at the desired confluence and transiently transfected with plasmids using Lipofectamine 2000 (Invitrogen) according to the manufacturer's instructions. After 20–24 h, the cells were fixed in 4% PFA for 15 min at room temperature, washed with PBS, permeabilized with 0.3% Triton X-100 in PBS for 15 min, washed with PBS, and blocked for 1 h in blocking buffer (PBS containing 10% FBS, 5% BSA, 0.01% NaN3, and 0.2% Triton X-100) at room temperature.

Western blotting and co-immunoprecipitation

Immunoblotting

Isolated mouse cortices or HEK293T cells were lysed in cell lysis buffer (50 mM Tris-HCl, 150 mM NaCl, 1 mM EDTA, 1% NP40, pH 7.4) containing protease inhibitors. After sonication, the lysates were centrifuged at 13,000 × *g* for 10 min at 4°C, and protein concentrations in the collected supernatants were assessed by

bicinchoninic acid assay (BCA) using a Spectramax iD3 plate reader. The proteins were then separated by SDS–polyacrylamide gel electrophoresis, transferred onto nitrocellulose membranes (Millipore, Bedford, MA, USA) using a Pyxis Gel Processor, blocked with 5% (*m*/*v*) skimmed milk for 1 h at room temperature, and incubated with primary antibodies diluted in PBS containing 5% BSA and 0.1% NaN_3 at 4°C overnight. The next day, the membranes were washed three times with TBS, 10 min each wash, and then incubated with secondary antibodies at room temperature for 1 h.

Co-immunoprecipitation

For endogenous co-IP, cerebral cortices freshly dissected from E14.5 mouse embryos were lysed in cell lysis buffer (50 mM NaCl, 0.5% NP-40, 10 mM HEPES, 0.5 mM EDTA, 20 mM Tris, pH 7.4) supplemented with Complete Protease Inhibitor Tablets (Roche Applied Science) and 1 mM PMSF. Cell debris was pelleted at 13,000 rpm for 10 min at 4°C and the cell lysates were subjected to IP using protein A/G beads pre-incubated with antibodies against KCTD10 (PA553138, Invitrogen) or KCTD13 (HPA043524, Sigma) and rabbit IgG (PM035, MBL) at 4°C for 1.5 h with gentle rotation. Immunoprecipitates were washed 3-5 times with cell lysis buffer, eluted with 2 × SDS sample buffer, and analyzed by SDS–PAGE as described above.

For exogenous co-IP, HEK293T cells were transfected with equal amounts of the indicated plasmids using VigoFect (Vigorous Biotechnology Beijing Co., Ltd.). After 24 h, the transfected cells were lysed in cell lysis buffer (50 mM NaCl, 0.5% NP-40, 10 mM HEPES, 0.5 mM EDTA, 20 mM Tris, pH 7.4) supplemented with a protein inhibitor cocktail and incubated on ice for 30 min, with mixing by inversion every 10 min. After centrifugation, the supernatant was incubated with Flag-M2 beads at 4° C for 4 h with gentle rotation and mixing, or with anti-HA magnetic beads at 4°C overnight. The subsequent steps were the same as those used for endogenous co-IP.

Immunofluorescence Analysis

Embryonic mouse brains were dissected out and immediately fixed in 4% PFA overnight at 4° C. Brain tissues were subsequently transferred to 30% sucrose until completely dehydrated, embedded in optimum cutting temperature (OCT) compound, frozen at −80℃ for at least 2 h, and cryosectioned into 20 μm slices for immunostaining. For the majority of immunofluorescence staining, tissue sections were incubated for 1 h at room temperature in blocking buffer (10% horse serum and 5% BSA in PBS with 0.2% Triton X-100) containing 0.01% NaN3 and then incubated with primary antibodies diluted in the same blocking buffer at 4°C overnight. After washing three times with 0.2% Triton X-100 in PBS, the brain sections were incubated with the appropriate fluorescent-labeled secondary antibodies diluted in blocking buffer for 1 h at room temperature, washed three times with 0.2% Triton X-100 in PBS, and counterstained with DAPI at room temperature for 10 min. Images were acquired with a confocal laser scanning microscope (Leica SP8 and Zeiss LSM 980).

Grip force measurement

The grip force test is utilized to measure the grip force of the forelimbs or all limbs. Grip force was assessed using a digital grip strength meter (Ugo Basile 47200), equipped with a fine metal grid fixed on the sensor. During the test, each mouse was lifted by the tail and encouraged to grip horizontal rigid grids linked to a digital force gauge. Subsequently, the tail was gently pulled backward horizontally while maintaining the mouse's body parallel to the grid. The peak tension value recorded on the digital force gauge represented the maximum grip strength exerted until the mouse released its grasp. The reported value for each mouse is an average of three test attempts, with a 5-minute rest period between each test.

Footprint analysis

Footprint analysis was conducted to examine the gait patterns of mice using a 70 cm long and 7 cm wide flat passageway. Red and blue pigments were applied to the mice's forelimbs and hind limbs, respectively. Following acclimation to the

designated pathway, the mice aged P19 or P23 were allowed to walk freely in the passageway. The step stances, including the stride length of the left hind limb, left forelimb, right hind limb, and right forelimb, as well as the forelimb stance and hind limb stance, were measured. Each index required an average of more than 6 steps for statistical analysis.

Open field test

Wild-type (WT) or *Kctd10* cKO mice aged P20 or P23 were individually placed at the center of a 72 cm × 72 cm × 40 cm open-field arena. Their movement trajectories were recorded for 30 minutes using the Smart V3.0 behavioral analysis software. The total movement distance, resting duration, and rearing duration were then calculated. Before commencing each subsequent trial, the open-field arena was thoroughly cleaned with 75% ethanol.

Cylinder test

Wild-type (WT) or *Kctd10* cKO mice at P20 were placed in a transparent plexiglass cylinder measuring 20 cm in diameter and 40 cm in height, and their movements were recorded from top to bottom for 15 minutes. After the test, the mice were returned to their original cage, and the apparatus was cleaned before the next mouse was tested. Subsequently, the duration and frequency of standing were quantified.

***In utero* electroporation**

In utero electroporation was conducted as previously reported(1), with minor modifications. In brief, on E13.5 or E14.5, pregnant ICR mice were deeply anesthetized with 2,2,2-tribromoethanol (30 mg/kg body weight) in tert-amyl alcohol. Plasmid DNA (2–3 mg/mL) was mixed with 0.2% Fast Green (2 mg/mL; Sigma) and was randomly microinjected into one fetal lateral ventricle through a polished glass micropipette (Drummond). Throughout the procedure, the uterus was kept moist by applying pre-warmed normal saline dropwise. Five pulses of current (30 mV for 50 ms, 950 ms interval) were delivered across the head of the embryos with a 7-mm diameter Tweezertrode Electrode (BTX Harvard Apparatus) using an electroporator

(ECM-830 BTX, Harvard Apparatus). At the corresponding time, the embryos were dissected for phenotypic analysis.

Neurosphere culture

Neural progenitors were isolated from the cerebral cortex of E14.5 embryos. After harvesting, the embryos were placed in pre-cooled PBS, and the brains were dissected and transferred to a 6-cm-diameter dish containing HBSS. Once the meninges and cerebral nuclei had been peeled off, the cerebral cortex was isolated and fully digested with moderate papain at 37°C for 30 min (with shaking once every 5–10 min). Digestion was terminated by adding 1 mL of DMEM containing 10% FBS. After centrifugation, the resulting cell pellets were washed three times with proliferation medium (DMEM/F12 supplemented with 2% B27, 20 ng/mL basic fibroblast growth factor, 200 ng/mL epidermal growth factor, and 1% penicillin–streptomycin). Finally, the neural progenitors were inoculated in 6-well plates at a density of 5×10^4–1×10^5 cells/mL and cultured at 37°C with 5% CO_2.

RNA extraction and real-time PCR

Total RNA was procured using Trizol reagent (Invitrogen). One microgram of total RNA was utilized for cDNA synthesis with the iScript reverse transcriptase (Vazyme). Real-time PCR was conducted using the Power SYBR Green PCR Master Kit (Thermo Scientific) on a CFX96 (Bio-RAD). Expression data were normalized to the mean of the housekeeping gene *Gapdh*. For *Kctd13*, two pairs of primers spanning different exons were employed. The primer sequences are as follows:

Kctd13 (exon 4-5): Fw 5′-ACACAACCGCAGTAACAACA,

Rv 5′-CGTAGAAAGACCAGCAGCAA;

Kctd13 (exon 5-6): Fw 5′-TTGCTGCTGGTCTTTCTACG,

Rv 5′-GCCACGGGAATTCTCATAAA;

Gapdh: Fw 5′- ATCCCAGAGCTGAACGGGAAGC,

Rv 5′- TTGGGGGTAGGAACACGGAAGG.

Bioinformatics

Gene Ontology (GO) analysis was conducted for highly correlated genes (|Spearman's correlation coefficient| > 0.7) with *KCTD10* or DEPs identified in quantitative MS utilizing the Database for Annotation, Visualization, and Integrated Discovery (DAVID) website (https://david.ncifcrf.gov/). Significantly enriched GO terms were filtered by a P value below 0.05.

References

1. Saito T (2006) In vivo electroporation in the embryonic mouse central nervous system. *Nat Protoc* 1(3):1552-1558.

Figure S1

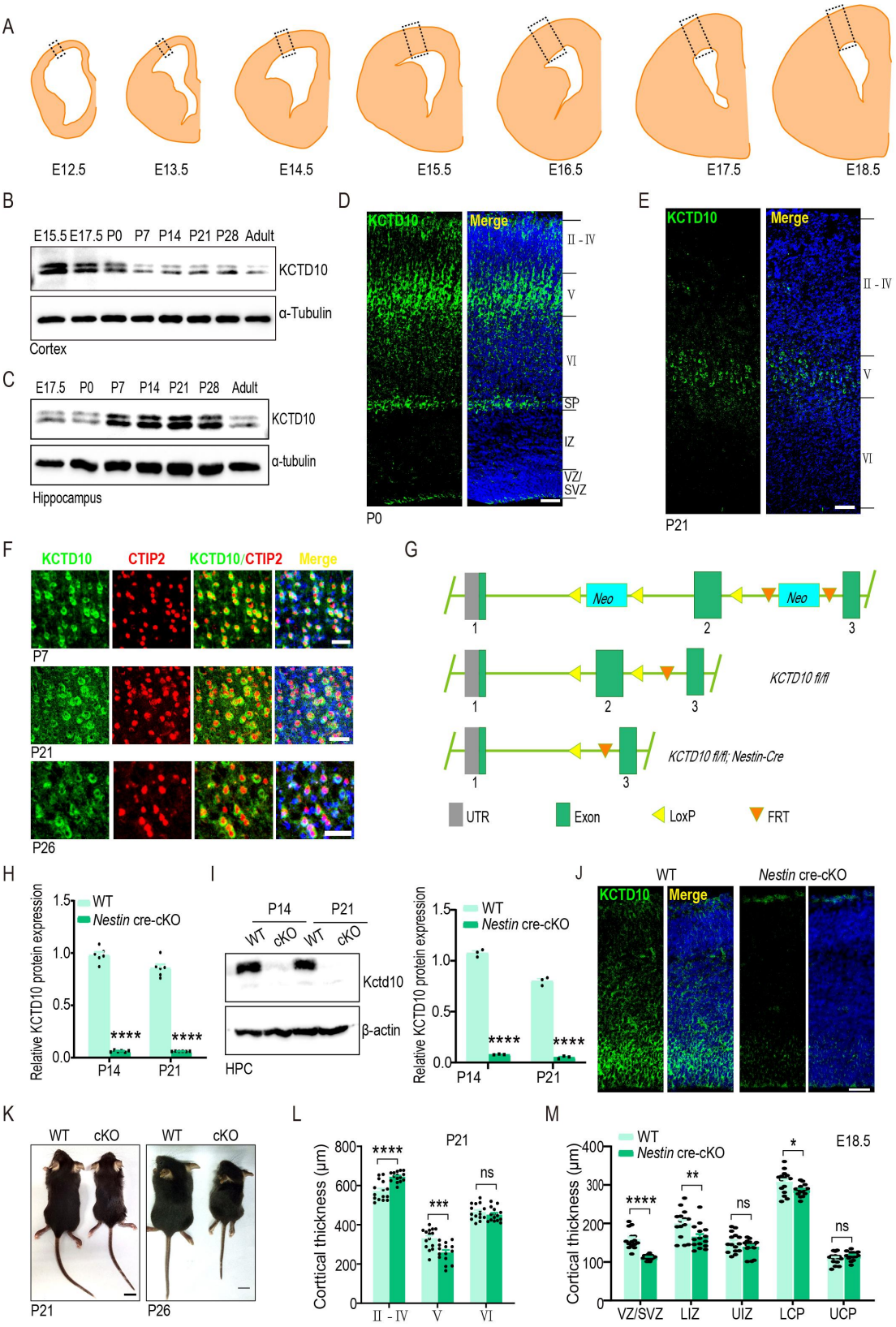
A
E12.5
E13.5
E14.5
E15.5
E16.5
E17.5
E18.5
B
E15.5 E17.5 P0 P7 P14 P21 P28 Adult
KCTD10
α-Tubulin
Cortex
C
E17.5 P0 P7 P14 P21 P28 Adult
KCTD10
α-tubulin
Hippocampus
D
KCTD10
Merge
II - IV
V
VI
SP
IZ
VZ/SVZ
P0
E
KCTD10
Merge
II - IV
V
VI
P21
F
KCTD10
CTIP2
KCTD10/CTIP2
Merge
P7
P21
P26
G
Neo
Neo
1
2
3
KCTD10 fl/fl
KCTD10 fl/fl; Nestin-Cre
UTR
Exon
LoxP
FRT
H
WT
Nestin cre-cKO
Relative KCTD10 protein expression
1.5
1.0
0.5
0.0
****
****
P14
P21
I
P14
P21
WT
cKO
WT
cKO
Kctd10
β-actin
HPC
Relative KCTD10 protein expression
WT
Nestin cre-cKO
****
****
P14
P21
J
WT
Nestin cre-cKO
KCTD10
Merge
K
WT
cKO
WT
cKO
P21
P26
L
P21
Corttical thickness (μm)
800
600
400
200
0
****
***
ns
II - IV
V
VI
M
E18.5
WT
Nestin cre-cKO
Cortical thickness (μm)
400
300
200
100
0
****
**
ns
*
ns
VZ/SVZ
LIZ
UIZ
LCP
UCP

Fig. S1. KCTD10 plays an important role in brain development, related to Fig. 1.
(*A*) E12.5-E18.5 cortices from rostral regions shown in all figures. (*B*, *C*) Western blotting analysis of cerebral cortex and hippocampus lysates from various developmental stages were analyzed by immunoblotting with KCTD10 antibody. α-tubulin was used as a loading control. (*D*, *E*) Representative images of P0 (*D*) and P21 (*E*) cortices stained for KCTD10 (green) and DAPI (blue). (*F*) Enlarged images of P7, P21, and P26 cortices stained for KCTD10 (green), CTIP2 (red), and DAPI (blue). (*G*) Gene targeting strategy for *Kctd10* cKO mice. The 2nd exon is flanked by two LoxP sequences (yellow triangles). UTR, untranslated region; Neo, selection marker; The FLP recombinase recognizes the FRT sites and excises the DNA fragment between them when FRT sites are in the same orientation. (*H*) Quantification of Figure 1F. Relative KCTD10 expression in the cortex of WT and cKO mice at P14 and P21. WT and cKO: *n*=6. (*I*) Western blotting results showing loss of KCTD10 in the hippocampus of *Nestin*-cKO mice at P14 and P21. β-Actin was used as a loading control. Relative protein expression of KCTD10 (right panel). WT and cKO: *n*=3. (*n*, brain numbers). (*J*) Representative images of WT and *Kctd10* cKO cortices on E14.5 stained for KCTD10 (green) and DAPI (blue). (*K*) Representative images of WT and *Kctd10* cKO mice at P21 and P26. (*L*) Quantification of cortical thickness on P21 in Fig. 3*C*. WT and cKO: *n*=15/5. (*M*) Quantification of cortical thickness on P21 in Fig. 1*J*. WT and cKO: *n*=15/5. All data are mean±SEM (error bars). Student's *t*-test. **P*<0.05, ***P*<0.01, ****P*<0.001,****P<0.0001. Scale bars: 50 μm (*D*, *F*, *J*), 100 μm (*E*), and 2 mm (*K*).

Figure S2

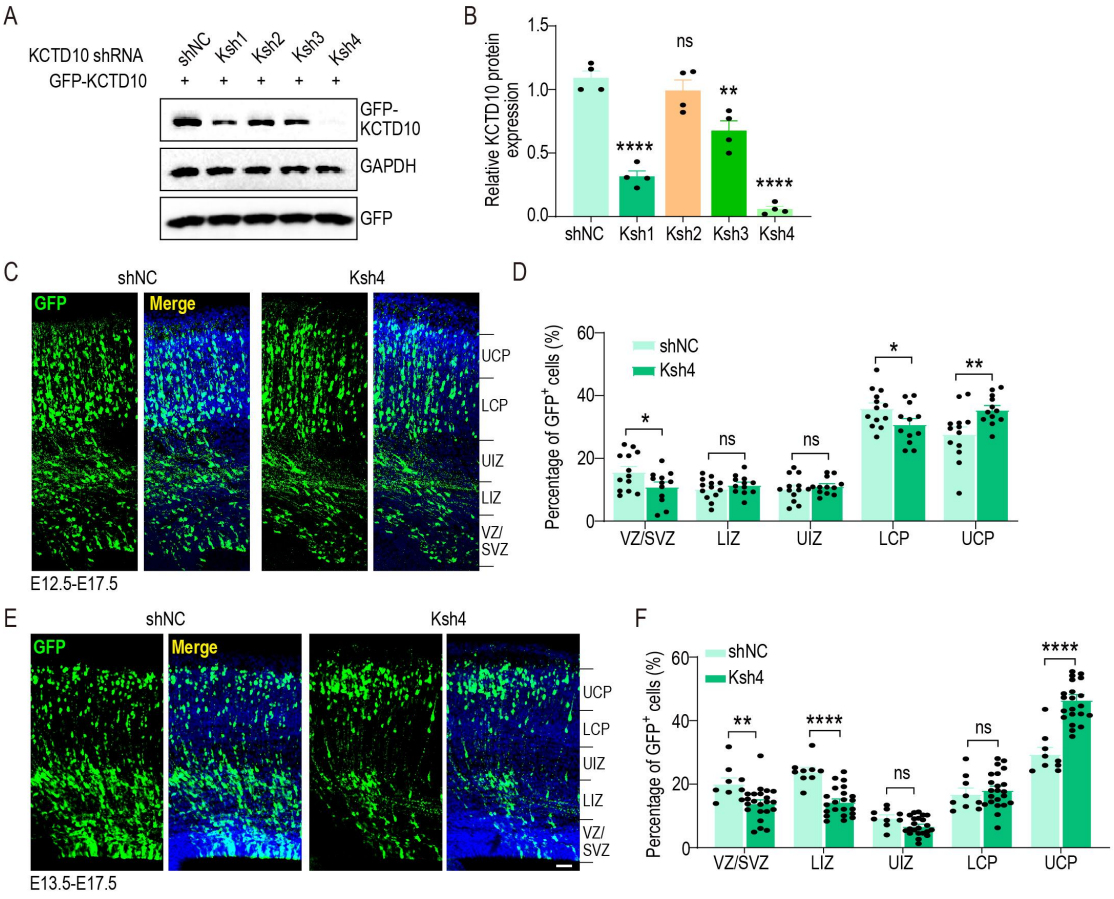

Fig. S2. KCTD10 knockout affects the cellular distribution in the developing cortex, related to Fig. 1.
(*A*) Knockdown efficiency of shRNAs targeting *Kctd10* confirmed by Western blotting. (*B*) Quantification of (*A*). Relative KCTD10 expression when GFP- KCTD10 co-transfected with control (shNC) or *Kctd10* shRNA (Ksh1-Ksh4) for 48h. *n*=3 from 3 independent experiments. (*C*) Representative images of E17.5 cortices electroporated on E12.5 with shNC or *Kctd10* shRNA4 (Ksh4). (*D*) Quantification of the percentage of transfected cells in each respective region. shNC: *n*=13/3, Ksh4: *n*=12/3. (*E*) Representative images from E17.5 cortices electroporated on E13.5 with shNC or *Kctd10* shRNA4 (Ksh4) and stained with GFP antibody, and DAPI (blue). (*F*) Quantification of the percentage of transfected cells in each region. shNC: *n*=9/3, Ksh4: *n*=22/6. All data are presented mean ± SEM (error bars). Student's *t*-test. ***P*<0.01, *****P*<0.0001, ns: no significance. Scale bars: 50 μm (*C*).

Figure S3

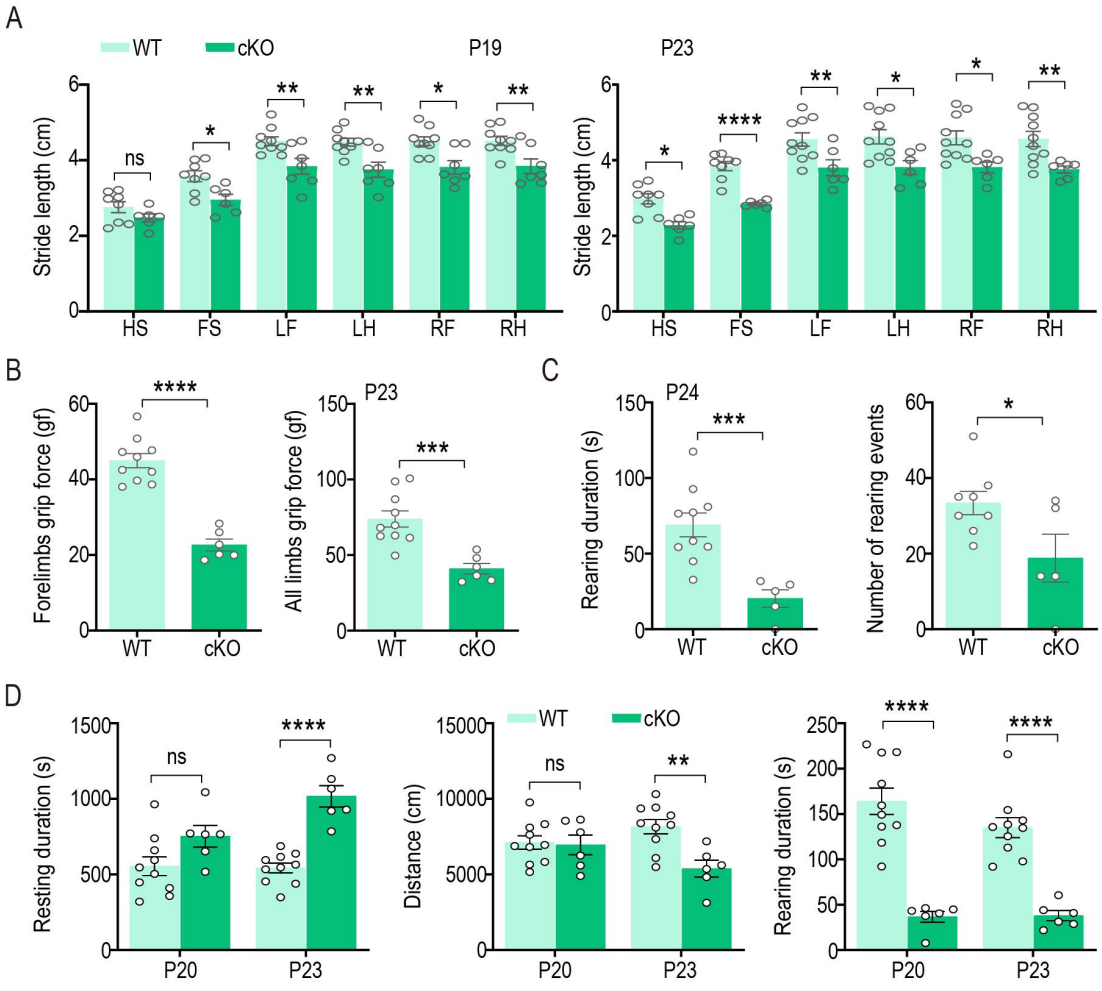

Fig. S3. *Kctd10* cKO mice exhibit motor deficits, related to Fig. 1.
(*A*) Abnormal footprints detected in *Kctd10* cKO mice at both P19 and P23. The stride length (cm) and limb stance (left, right, hind limb and forelimb) were assessed using footprint tests. HS: Hind limb stance, FS: Forelimb stance, LF: Left forelimb, LH: Left hind limb, RF: Right forelimb, RH: Right hind limb. WT: *n*=8, cKO: *n*=6 (*n*=mice numbers). (*B*) Comparison of grip force (gf: gram force) in the limbs of the WT and *Kctd10* cKO mice at P23. WT: *n*=10, cKO: *n*=6. (*C*) Comparison of the number and duration of rearing events analyzed in WT and *Kctd10* cKO mice during the cylinder experiment. WT: *n*=10, cKO: *n*=5. (*D*) Assessment of resting duration, rearing duration, and total moving distance during the open field assay. WT: *n*=10, cKO: *n*=6. All data are presented as mean ± SEM (error bars). Student's *t*-test. **P*<0.05, ***P*<0.01, ****P*<0.001, *****P*<0.0001, ns: no significance.

Figure S4

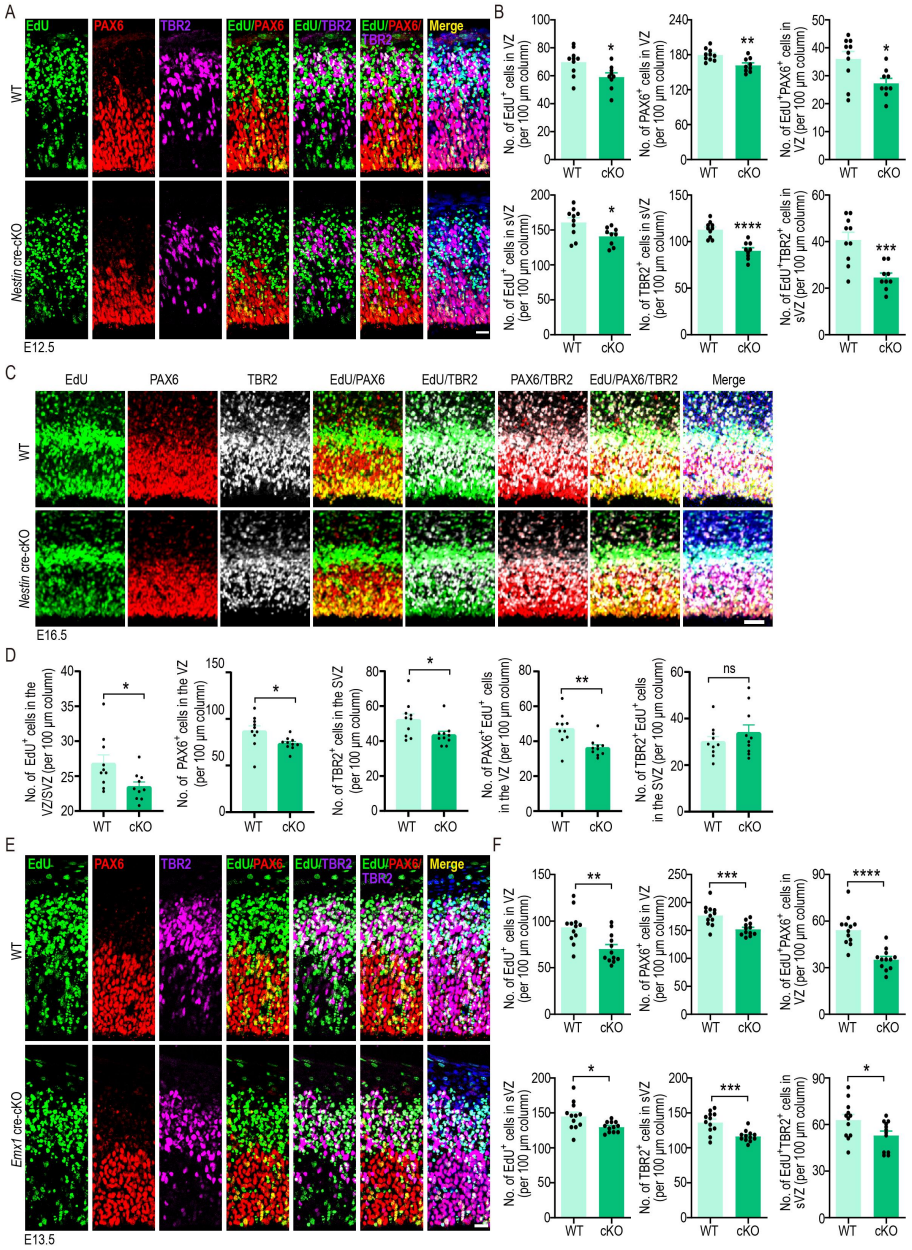

Fig. S4. *Kctd10* deficiency suppresses the proliferation of NPCs, related to Fig. 2.

(*A*) Representative images of E12.5 WT and *Kctd10* Nestin-cre cKO mouse cortices stained for EdU (green), PAX6 (red), TBR2 (magenta) and with DAPI (blue). EdU was administered at E11.5. (*B*) Quantification of the number of EdU^+ cells and $PAX6^+$ cells in the VZ, EdU^+ cells and $TBR2^+$ cells in the SVZ, EdU^+PAX6^+ in the VZ, and EdU^+TBR2^+ in the SVZ per 100 μm column in (*A*). WT: *n*=10/3, cKO: *n*=9/3. (*C*) Representative images of E16.5 WT and *Kctd10* cKO mouse cortices stained for EdU (green), PAX6 (red), TBR2 (gray), and with DAPI (blue). EdU was injected at E15.5. (*D*) Quantification of the number of EdU^+ cells in the VZ/SVZ, $PAX6^+$ cells in the VZ, $TBR2^+$ cells in the SVZ, EdU^+PAX6^+ in the VZ, and EdU^+TBR2^+ in the SVZ per 100 μm column in (*C*). WT, cKO: *n*=10/3. (*E*) Representative images of E13.5 WT and *Kctd10 EMX1* cre cKO mouse cortices stained for EdU (green), PAX6 (red), TBR2 (magenta), and counterstained with DAPI (blue). EdU labeling was performed following injection at E12.5. (*F*) Quantification of the number of EdU^+, $PAX6^+$, EdU^+PAX6^+ cells in the VZ, EdU^+, $TBR2^+$, and EdU^+TBR2^+ cells in the SVZ per 100 μm column in (*E*). WT, cKO: *n*=12/4. All data are mean±SEM. Student's *t*-test. **P*<0.05, ***P*<0.01, ****P*<0.001, *****P*<0.0001. *n*=slice/brain numbers. Scale bars: 50 μm (*C*), 20 μm (*A, E*).

Figure S5

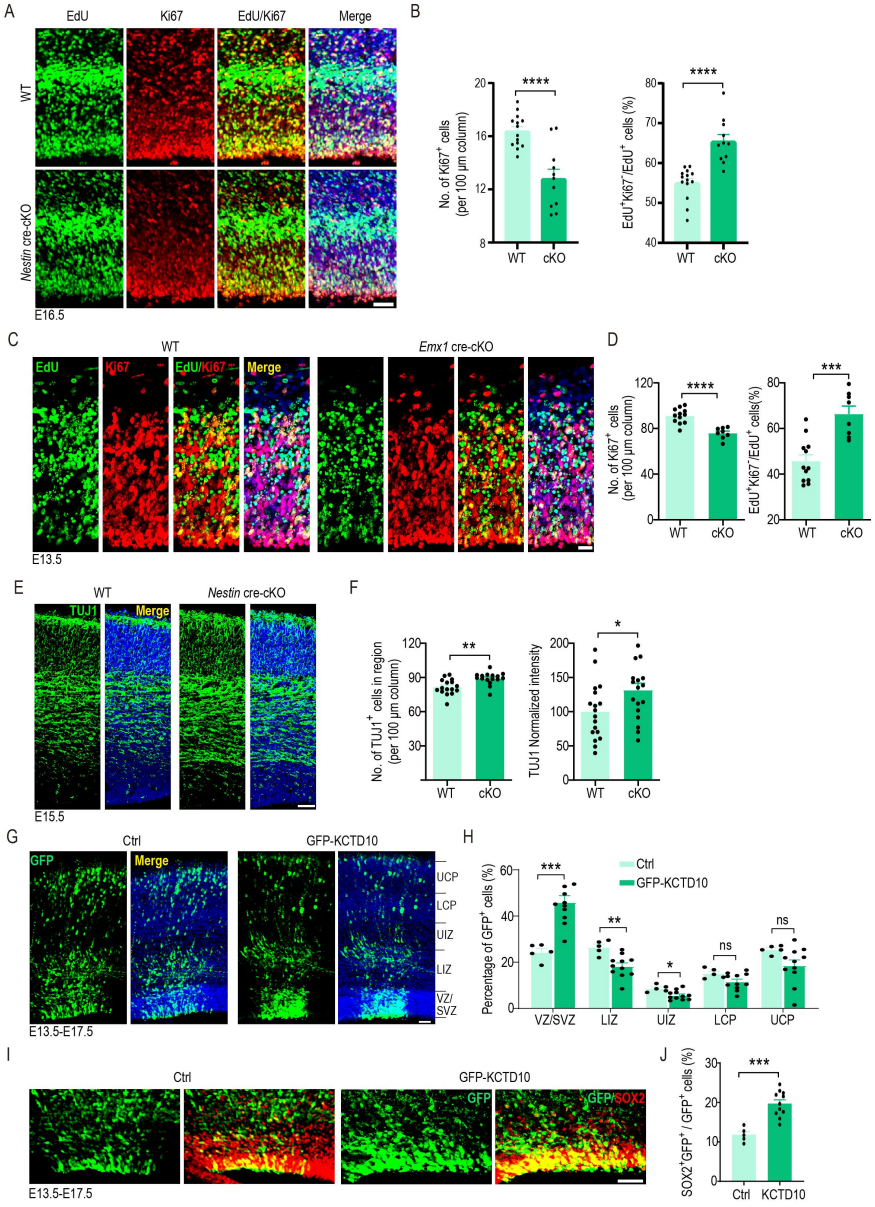

Fig. S5. *Kctd10* deficiency leads to premature differentiation of NPCs, related to Fig. 2.

(*A*) Representative images of E16.5 WT and *Kctd10* cKO cortices stained for EdU (green), Ki67 (red), and with DAPI (blue). (*B*) Quantification of the number of $Ki67^+$ cells per 100 μm column and the percentage of EdU^+Ki67^-/EdU^+ cells represented exiting the cell cycle. WT, cKO: *n*=10/3. *(C)* Representative images of E13.5 WT and *Kctd10 EMX1* cre-cKO cortices stained for EdU (green), Ki67 (red), and with DAPI (blue). *(D)* Quantification of the number of $Ki67^+$ cells per 100 μm column and the percentage of EdU^+Ki67^-/EdU^+ cells represented exiting the cell cycle. WT: *n*=12/4, cKO: *n*=8/3. *(E)* Representative images of E15.5 WT and *Kctd10* cKO cortices stained for TUJ1 (green) and with DAPI (blue). *(F)* Quantification of the number of $TUJ1^+$ cells per 100μm column and normalized intensity of TUJ1. WT, cKO: *n*=16/4. *(G)* Representative images are from E17.5 cortices electroporated on E13.5 with empty vector (Ctrl) or GFP-KCTD10 and stained with GFP antibody and DAPI (blue). (*H*) Quantification of the percentage of GFP^+ cells in the VZ/SVZ, LIZ, UIZ, LCP and UCP in *(G)*. Ctrl: *n*=5/3, GFP-KCTD10: *n*=11/4. *(I)* Representative images are from E17.5 cortices electroporated on E13.5 with empty vector (Ctrl) or GFP-KCTD10 and stained with indicated antibodies. (*J*) Quantification of the percentage of GFP^+SOX2^+/GFP^+ cells in the VZ/SVZ. Ctrl: *n*=5/3, GFP-KCTD10: *n*=11/4. *n*=slice/brain numbers. All data are mean±SEM. Student's *t*-test. **P*<0.05, ***P*<0.01, ****P*<0.001, *****P*<0.0001. *n*=slice/brain numbers. Scale bars: 50 μm (*A*, *E*, *G, I*), 20 μm (*C*).

Figure S6

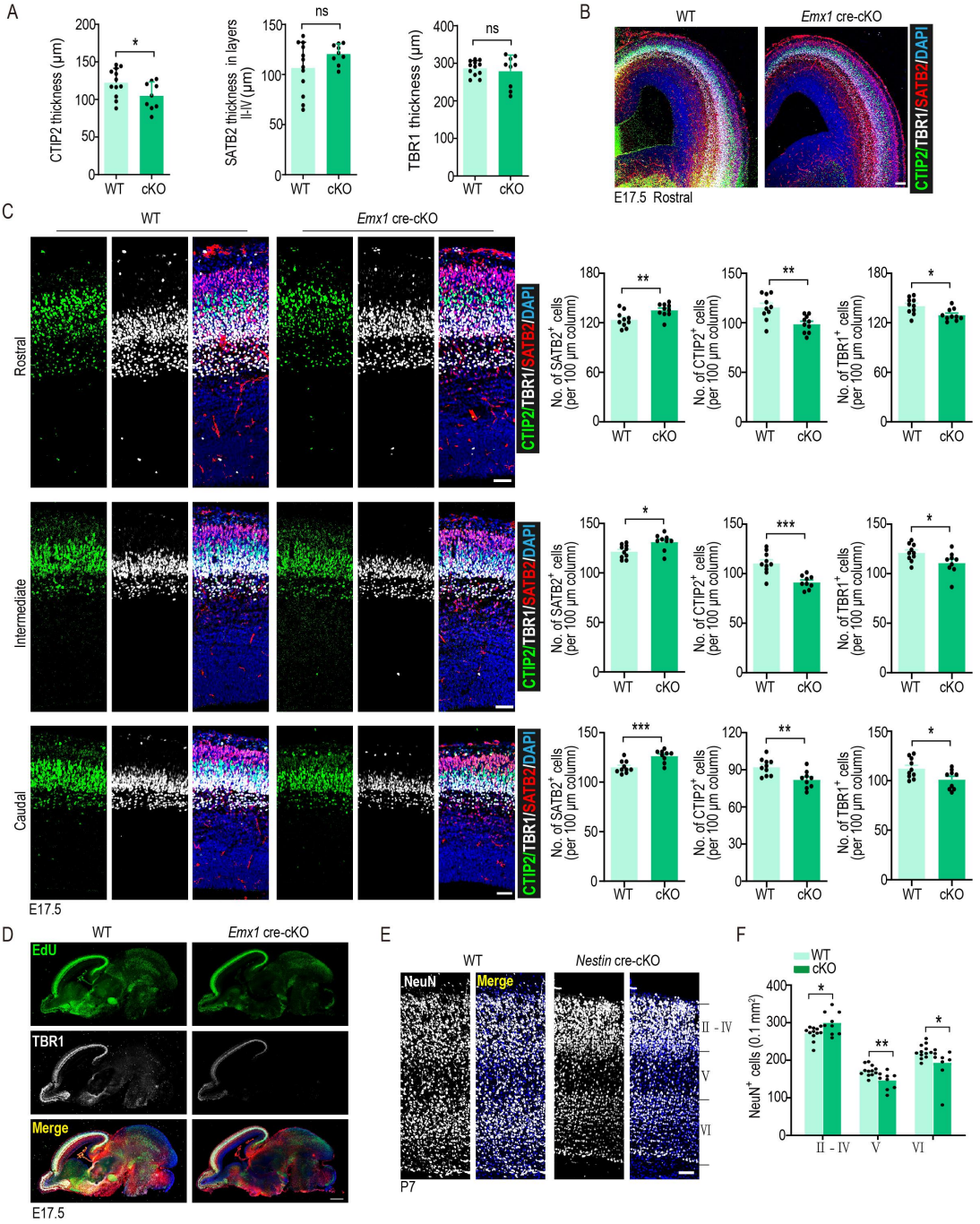

Fig. S6. KCTD10 knockout affects the production of cortical neurons, related to Fig. 3.
(*A*) Quantification of the thickness of SATB2$^+$, CTIP2$^+$ and TBR1$^+$ neuronal layers in Fig. 3*A*. CTIP2 (WT: *n*=12/4, cKO: *n*=9/3), TBR1 and SATB2 (WT: *n*=12/4, cKO: *n*=9/3). (*B*) E17.5 cortices from rostral regions of WT and cKO embryos shown in (*C*) were co-stained for CTIP2 (green), TBR1 (gray), SATB2 (red) and DAPI (blue). (*C*) E17.5 cortices from rostral, intermediate and caudal regions of WT and cKO embryos co-stained for CTIP2 (green), TBR1 (gray), SATB2 (red) and DAPI (blue). WT: *n*=10/3, cKO: *n*=10/3 (roatral), cKO: *n*=9/3 (intermediate and caudal). (*D*) Representative sagittal sections of E17.5 WT and cKO brains immnuno-stained for CTIP2 (green), TBR1 (gray), SATB2 (red) and DAPI (blue). (*E*) Representative coronal sections of P7 WT and cKO brains stained for NeuN (gray). (*F*) Quantification of NeuN$^+$ cells per 0.1 mm^2 in (*E*). WT: *n*=12/4, cKO: *n*=9/3. All data are mean ± SEM. Student's *t*-test. **P*<0.05, ***P*<0.01. ns: no significance. *n* = slice/brain numbers. Scale bars: 50 μm (*C*), 100 μm (*B, E*), 500 μm (*D*).

Figure S7

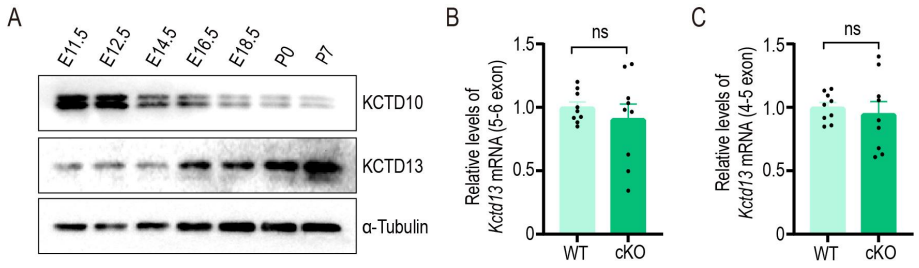

Fig. S7. *Kctd10* loss has no effects on *Kctd13* mRNA level, related to Fig. 5.
(*A*) Western blotting analysis of cerebral cortex lysates from various developmental stages were analyzed by immunoblotting with KCTD10 and KCTD13 antibody. α-tubulin was used as a loading control. (*B*, *C*) The mRNA levels of *Kctd13* in the cerebral cortex of WT and *Kctd10* cKO mouse at E13.5 were determined by Real-time PCR using two different primers spanning exon 5 and 6 or exon 4 and 5.*β-Actin* was used as an internal control. All data are presented as mean ± SEM. Student's *t*-test. ns: no significance.

Figure S8

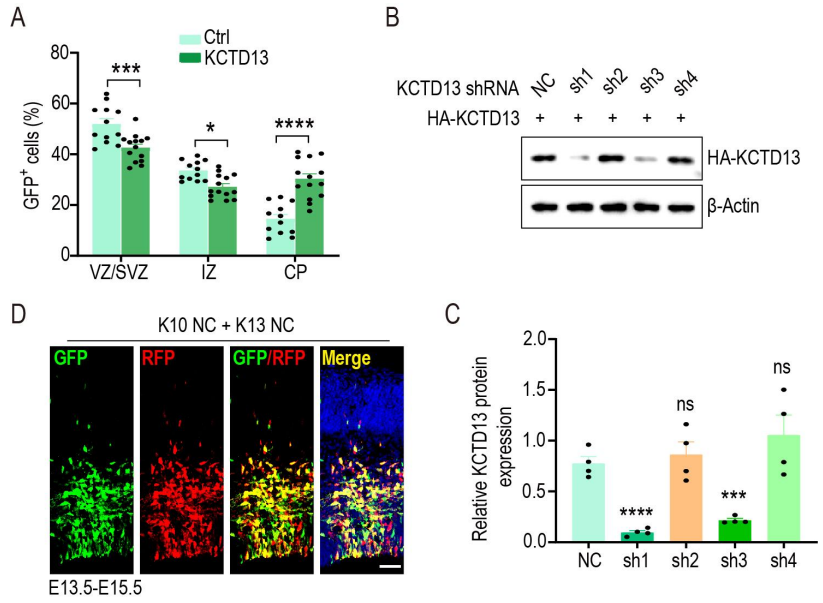

Fig. S8. Overexpression of KCTD13 leads to abnormal cell distribution in the developing cortex, related to Fig. 6.
(*A*) Quantification of the percentage of GFP$^+$ cells in the VZ/SVZ, IZ or CP. Ctrl: *n*=12/3, HA-KCTD13: *n*=14/4. *n*=slice/brain numbers. (*B*) Knockdown efficiency of *Kctd13* targeting shRNAs confirmed by Western blot analysis. *(C)* Quantification of (*B*). Relative KCTD13 expression when HA - KCTD10 co-transfected with negative control (NC) or *Kctd13* shRNA (sh1-sh4) for 48 hours. *n*=3 from 3 independent experiments. *(D)* Representative images from E15.5 cortices electroporated on E13.5 with GFP fused K10 NC and RFP fused K13 NC stained with GFP, RFP antibody, and DAPI (blue). Almost all transfected cells were both GFP and RFP positive. Scale bar: 50 μm. All data are presented as mean ± SEM. Student's *t*-test. **P*<0.05, ****P*<0.001, *****P*<0.0001. ns: no significance.

288 **Table S1. Unique proteins pulled down by the KCTD10 antibody**

Protein name	Gene name	Protein score	Sequence coverage (%)	No. specific peptides	No. peptides	No. secondary spectra	Abundance
Hsc70-interacting protein	St13	788	33	13	13	25	2.13E+09
AP-1 complex subunit beta-1	Ap1b1	760	20	5	13	19	9.61E+06
Epidermal growth factor receptor substrate 15	Eps15	424	18	11	11	12	2.89E+07
Keratin, type II cytoskeletal 6A	Krt6a	384	12	2	8	13	2.55E+07
BTB/POZ domain-containing adapter for CUL3-mediated RhoA degradation protein 3	Kctd10	329	20	6	8	12	6.69E+07
Keratin, type I cytoskeletal 17	Krt17	307	18	1	10	12	1.81E+08
Centrosomal protein of 112 kDa	Cep112	242	11	7	7	8	1.28E+07
Fibrinogen beta chain	Fgb	217	16	5	5	5	2.13E+07
Flavin reductase (NADPH)	Blvrb	212	23	3	3	4	5.47E+06
DNA damage-binding protein 1	Ddb1	184	5	4	4	4	7.11E+06
14-3-3 protein beta/alpha	Ywhab	169	23	1	6	6	2.66E+06
Keratin, type I cytoskeletal 19	Krt19	163	9	1	5	5	3.88E+06
BTB/POZ domain-containing adapter for CUL3-mediated RhoA degradation protein 1	Kctd13	162	20	3	5	5	9.08E+06
Sodium/potassium-transporting ATPase subunit alpha-1	Atp1a1	149	6	2	4	4	1.09E+07
Histone H2A type 3	H2aw	144	35	2	4	5	5.84E+08
Rabphilin-3A	Rph3a	135	15	5	5	5	1.21E+07
ELAV-like protein 2	Elavl2	132	13	1	5	5	2.74E+06
BTB/POZ domain-containing protein 9	Btbd9	125	8	3	3	3	2.55E+06
Keratin, type II cuticular Hb4	Krt84	123	5	1	4	5	1.97E+06
Exopolyphosphatase PRUNE1	Prune1	119	11	3	3	3	4.78E+06
DnaJ homolog subfamily B member 1	Dnajb1	116	13	4	4	4	8.96E+06
Traf2 and NCK-interacting protein kinase	Tnik	112	3	1	5	5	2.83E+06
5'-3' exoribonuclease 2	Xrn2	108	3	2	2	2	5.39E+05

Pre-mRNA-processing factor 6	Prpf6	106	4	3	3	3	5.70E+06
DAZ-associated protein 1	Dazap1	100	8	2	2	2	5.08E+06
Tenascin-R	Tnr	100	2	2	2	2	1.93E+06
Protein TSSC4	Tssc4	99	8	2	2	2	4.56E+06
ATP-dependent RNA helicase DHX30	Dhx30	97	3	3	3	3	3.15E+06
Coiled-coil domain-containing protein 177	Ccdc177	94	3	2	2	2	3.82E+06
Serine/threonine-protein phosphatase 6 regulatory subunit 2	Ppp6r2	90	6	4	4	4	6.08E+06
Elongation factor 1-delta	Eef1d	89	9	2	2	2	6.32E+06
Kinesin-1 heavy chain	Kif5b	88	3	2	2	2	3.77E+06
Fibrinogen alpha chain	Fga	84	3	3	3	3	9.86E+06
Fibrinogen gamma chain	Fgg	82	12	4	4	4	1.17E+07
Eukaryotic initiation factor 4A-II	Eif4a2	81	10	1	3	3	2.50E+06
Ferritin light chain 2	Ftl2	79	9	1	1	1	1.70E+06
Ig kappa chain V-V region T1	Ig	76	18	2	2	2	1.98E+07
Methionine aminopeptidase 2	Metap2	74	9	3	3	3	3.92E+06
AP-1 complex subunit mu-1	Ap1m1	74	9	3	3	3	4.96E+06
Dynamin-1-like protein	Dnm1l	74	6	4	4	4	6.01E+06
RNA 3'-terminal phosphate cyclase	RtcA	74	4	1	1	1	1.01E+06
CLIP-associating protein 2	Clasp2	71	3	2	4	4	3.11E+06
Ig heavy chain V region VH558 A1/A4	Gm5629	70	13	1	1	1	2.82E+06
Alpha-1,3/1,6-mannosyltransferase ALG2	Alg2	70	3	1	1	1	2.39E+06
26S proteasome regulatory subunit 7	Psmc2	65	3	1	1	1	8.17E+05
Apoptosis regulator BAX	Bax	63	7	1	1	1	1.17E+06
CD2 antigen cytoplasmic tail-binding protein 2	Cd2bp2	62	7	2	2	2	5.59E+06
Formin-like protein 3	Fmnl3	58	3	2	2	2	3.54E+06
ATP-binding cassette sub-family E member 1	Abce1	57	3	1	1	1	2.94E+05
Apoptosis inhibitor 5	Api5	56	4	1	1	1	1.36E+06
Centrosomal protein of 170 kDa	Cep170	56	1	1	1	1	1.28E+06
ATP-dependent RNA helicase DDX19A	Ddx19a	56	6	2	2	2	5.61E+05

Lysine--tRNA ligase	Kars1	55	5	2	2	2	3.32E+06
U1 small nuclear ribonucleoprotein C	Snrpc	54	8	1	1	2	1.74E+06
Histone H3.3	H3-3a	53	12	2	2	2	1.17E+08
40S ribosomal protein S15	Rps15	52	7	1	1	1	1.97E+06
RuvB-like 1	Ruvbl1	50	4	1	1	1	5.45E+05
Beta-adducin	Add2	50	2	1	1	1	1.14E+06
26S proteasome non-ATPase regulatory subunit 11	Psmd11	46	3	1	1	1	1.10E+06
Glutathione peroxidase 1	Gpx1	46	7	1	1	1	2.76E+06
Serine/threonine-protein phosphatase 4 regulatory subunit 3B	Ppp4r3b	44	3	2	2	2	1.89E+06
Zinc finger CCCH domain-containing protein 15	Zc3h15	43	3	1	1	1	1.50E+06
Phosphoribosyl pyrophosphate synthase-associated protein 2	Prpsap2	43	4	1	1	1	2.52E+05
Integrator complex subunit 3	Ints3	41	2	1	1	1	7.12E+05
ATP-dependent RNA helicase DHX29	Dhx29	40	1	1	1	1	3.56E+05
Eukaryotic translation initiation factor 1A, X-chromosomal	Eif1ax	40	5	1	1	1	8.21E+05
Non-histone chromosomal protein HMG-14	Hmgn1	39	9	1	1	1	4.91E+05
GTP-binding nuclear protein Ran	Ran	39	6	1	1	1	1.88E+06
26S proteasome non-ATPase regulatory subunit 12	Psmd12	39	3	1	1	1	1.40E+06
Transcription elongation regulator 1	Tcerg1	39	1	1	1	1	3.52E+06
Serine/threonine-protein phosphatase 4 regulatory subunit 2	Ppp4r2	37	4	1	1	1	1.63E+06
Serine/threonine-protein phosphatase 6 regulatory ankyrin repeat subunit A	Ankrd28	37	1	1	1	1	1.88E+06
Unconventional myosin-Ib	Myo1b	37	2	2	2	2	1.96E+06
DnaJ homolog subfamily C member 2	Dnajc2	37	2	1	1	1	7.09E+05
Serine/threonine-protein kinase BRSK1	Brsk1	36	2	1	1	1	1.22E+06
High affinity cAMP-specific and IBMX-insensitive 3',5'-cyclic phosphodiesterase 8B	Pde8b	35	1	1	1	1	2.98E+07

Very-long-chain (3R)-3-hydroxyacyl-CoA dehydratase 3	Hacd3	34	3	1	1	1	7.82E+05
B-cell receptor-associated protein 31	Bcap31	34	3	1	1	1	1.66E+06
Tropomyosin alpha-3 chain	Tpm3	33	5	1	1	1	2.08E+06
Glycerophosphocholine phosphodiesterase GPCPD1	Gpcpd1	33	1	1	1	1	6.93E+05
General transcription factor IIF subunit 1	Gtf2f1	33	2	1	1	1	3.31E+05
Protein PAT1 homolog 1	Patl1	33	2	1	1	1	7.98E+05
Ig heavy chain V region 3	Ighv1-61	33	21	1	1	1	1.73E+06
Ran-specific GTPase-activating protein	Ranbp1	32	3	1	1	1	1.88E+06
Transferrin receptor protein 1	Tfrc	32	1	1	1	1	8.62E+05
Proteasomal ubiquitin receptor ADRM1	Adrm1	32	4	1	1	1	1.31E+06
Mitogen-activated protein kinase 9	Mapk9	31	3	1	1	1	3.16E+05
Mitotic checkpoint protein BUB3	Bub3	31	3	1	1	1	8.47E+05
60S ribosomal protein L36	Rpl36	30	10	1	1	1	4.37E+06
WD40 repeat-containing protein SMU1	Smu1	30	2	1	1	1	1.77E+06
Protein SHQ1 homolog	Shq1	30	1	1	1	1	7.31E+06
Sister chromatid cohesion protein PDS5 homolog B	Pds5b	29	0	1	1	1	1.42E+06
NADH dehydrogenase [ubiquinone] iron-sulfur protein 8, mitochondrial	Ndufs8	29	5	1	1	1	1.45E+06
Protein SOGA3	Soga3	29	1	1	1	1	6.35E+06
Ig heavy chain V region 108A	Igh-VJ558	29	13	1	1	1	2.67E+06
WW domain-binding protein 11	Wbp11	28	1	1	1	1	1.64E+06
Lysine-specific demethylase 2A	Kdm2a	28	1	1	1	1	3.39E+06
Cytoplasmic FMR1-interacting protein 1	Cyfip1	28	1	1	1	1	4.86E+05
Mitogen-activated protein kinase 7	Mapk7	28	1	1	1	1	3.35E+06
Microtubule-associated protein 4	Map4	28	1	1	1	1	7.69E+05
AP-3 complex subunit beta-2	Ap3b2	27	1	1	1	1	8.47E+05
Polymerase delta-interacting protein 3	Poldip3	27	3	1	1	1	9.75E+05
Immunoglobulin-like domain-containing receptor 1	Ildr1	27	1	1	1	1	1.37E+07
Delta(14)-sterol reductase LBR	Lbr	27	1	1	1	1	1.12E+06

Vacuolar protein sorting-associated protein 51 homolog	Vps51	26	2	1	1	1	3.31E+05
Delta-1-pyrroline-5-carboxylate synthase	Aldh18a1	26	1	1	1	1	2.82E+06
PCI domain-containing protein 2	Pcid2	26	3	1	1	1	4.49E+05
Probable ATP-dependent RNA helicase DDX46	Ddx46	26	1	1	1	1	3.50E+05
Dynein light chain 2, cytoplasmic	Dynll2	26	12	1	1	1	1.68E+06
Putative acidic leucine-rich nuclear phosphoprotein 32 family member C	Anp32c	26	7	1	1	1	2.05E+06
Calcium/calmodulin-dependent protein kinase type II subunit alpha	Camk2a	26	1	1	1	1	2.10E+06
RAD52 motif-containing protein 1	Rdm1	25	2	1	1	1	1.69E+06
Cell division cycle and apoptosis regulator protein 1	Ccar1	25	1	1	1	1	2.38E+06
Lys-63-specific deubiquitinase BRCC36	Brcc3	25	3	1	1	1	6.42E+06
MAP/microtubule affinity-regulating kinase 3	Mark3	25	2	1	1	1	1.87E+05
ELKS/Rab6-interacting/CAST family member 1	Erc1	24	1	1	1	1	1.21E+06
Coatomer subunit beta'	Copb2	24	1	1	1	1	1.07E+06
RNA-binding protein 42	Rbm42	23	2	1	1	1	1.19E+06
Neurocan core protein	Ncan	23	1	1	1	1	1.49E+06
Zinc finger CCCH domain-containing protein 14	Zc3h14	23	1	1	1	1	2.42E+05
Putative sodium-coupled neutral amino acid transporter 11	Slc38a11	22	1	1	1	1	1.27E+06
Serine/arginine repetitive matrix protein 2	Srrm2	22	0	1	1	1	3.38E+05
Ras-related protein Ral-A	Rala	22	3	1	1	1	1.19E+06
Zinc finger C2HC domain-containing protein 1A	Zc2hc1a	22	6	1	1	1	1.12E+06
Eukaryotic translation initiation factor 5	Eif5	22	2	1	1	1	3.19E+05
Splicing factor 3B subunit 5	Sf3b5	21	17	1	1	1	8.07E+05
Protein enabled homolog	Enah	21	1	1	1	1	1.30E+06
mRNA cap guanine-N7 methyltransferase	Rnmt	21	3	1	1	1	1.21E+06

Target of EGR1 protein 1	Toe1	21	2	1	1	1	4.29E+05
Structural maintenance of chromosomes protein 1A	Smc1a	21	1	1	1	1	8.05E+05
Histone-lysine N-methyltransferase PRDM16	Prdm16	21	1	1	1	1	3.08E+06
Galectin-1	Lgals1	21	6	1	1	1	1.29E+06
Structural maintenance of chromosomes protein 3	Smc3	20	1	1	1	1	6.99E+05
Emerin	Emd	20	4	1	1	1	7.18E+05
AP-5 complex subunit zeta-1	Ap5z1	20	2	1	1	1	1.05E+07
YTH domain-containing family protein 3	Ythdf3	163	8	2	4	5	3.88E+06
Rho guanine nucleotide exchange factor 2	Arhgef2	80	2	1	1	1	1.74E+06
Exocyst complex component 4	Exoc4	76	3	2	2	2	1.80E+06
Nck-associated protein 1	Nckap1	49	2	2	2	2	2.73E+05
Regulatory-associated protein of mTOR	Rptor	38	1	1	1	1	4.83E+05
LanC-like protein 2	Lancl2	36	2	1	1	1	8.00E+05
Exosome complex component RRP45	Exosc9	29	2	1	1	1	1.72E+06
ATPase family AAA domain-containing protein 3	Atad3	27	2	1	1	1	1.94E+05

289

290

291

292

293

294

295

296

297

Table S2. Overlapping proteins obtained by quantitative MS and co-IP MS

Protein name	Gene name	Abundance (co-IP MS)	CKO/WT.Ratio	P.value (CKO/WT)
Fibrinogen alpha chain	Fga	9.86E+06	1.74996413	5.50E-05
Glutathione peroxidase 1	Gpx1	2.76E+06	1.227861483	4.86E-05
Galectin-1	Lgals1	1.29E+06	2.755501435	4.15E-07
Tropomyosin alpha-3 chain	Tpm3	2.08E+06	1.160962396	0.046823934
Transferrin receptor protein 1	Tfrc	8.62E+05	1.171176406	0.003990323
BTB/POZ domain-containing adapter for CUL3-mediated RhoA degradation protein 1	Kctd13	9.08E+06	1.186458881	0.005633296
Fibrinogen beta chain	Fgb	2.13E+07	1.545801945	4.08E-06
Fibrinogen gamma chain	Fgg	1.17E+07	1.513219403	9.69E-05
Structural maintenance of chromosomes protein 3	Smc3	6.99E+05	1.192566926	0.000203533
Apoptosis inhibitor 5	Api5	1.36E+06	1.179586773	8.15E-05
ATP-dependent RNA helicase DHX29	Dhx29	3.56E+05	1.284942405	0.000175989
Flavin reductase (NADPH)	Blvrb	5.47E+06	1.835790217	2.64E-05
Putative sodium-coupled neutral amino acid transporter 11	Slc38a11	1.27E+06	2.281971619	0.001833549
Protein SHQ1 homolog	Shq1	7.31E+06	2.709705777	0.02813395
High affinity cAMP-specific and IBMX-insensitive 3',5'-cyclic phosphodiesterase 8B	Pde8b	2.98E+07	0.798299227	0.00218633
Lysine-specific demethylase 2A	Kdm2a	3.39E+06	0.806639593	0.00313562
Traf2 and NCK-interacting protein kinase	Tnik	2.83E+06	0.832220956	0.001302252
Apoptosis regulator BAX	Bax	1.17E+06	0.760634071	0.045913535
Very-long-chain (3R)-3-hydroxyacyl-CoA dehydratase 3	Hacd3	7.82E+05	0.838229928	0.001794855
BTB/POZ domain-containing adapter for CUL3-mediated RhoA degradation protein 3	Kctd10	6.69E+07	0.821195785	0.027640455
AP-3 complex subunit beta-2	Ap3b2	8.47E+05	0.709429198	0.000116985
Beta-adducin	Add2	1.14E+06	0.84916056	0.00019716
Exopolyphosphatase PRUNE1	Prune1	4.78E+06	0.807888599	1.41E-05
Alpha-1,3/1,6-mannosyltransferase ALG2	Alg2	2.39E+06	0.630908318	0.000122994
AP-5 complex subunit zeta-1	Ap5z1	1.05E+07	0.815538645	0.004312429
Serine/threonine-protein phosphatase 6 regulatory subunit 2	Ppp6r2	6.08E+06	0.7760701	0.000151852
Coiled-coil domain-containing protein 177	Ccdc177	3.82E+06	0.803092387	0.001324082

Video S1.

Kctd10-cKO mice exhibited motor deficits.